Nano World Journal

https://doi.org/10.17756/nwj.2023-s5-027

Research Article

Open Access

Driving Capability Analysis and Power Supply Scaling Effects of Deep Nanoscale 1-bit Full Adder at Wide Operating Temperatures

Allamshetti Nikhitha, J. Ajayan, Bobbala Vaishanavi, Kummarikuntla Shivasai, Chandragiri Suchith Bhanu and B. Mounika*

Department of Electronics and Communications Engineering, SR University, Warangal, Telangana, India

***Correspondence to:**
B. Mounika
Department of Electronics and Communications Engineering,
SR University,
Warangal, Telangana, India.
E-mail: gmounika0509@gmail.com

Received: October 11, 2023
Accepted: December 19, 2023
Published: December 22, 2023

Citation: Nikhitha A, Ajayan J, Vaishanavi B, Shivasai K, Bhanu CS, et al. 2023. Driving Capability Analysis and Power Supply Scaling Effects of Deep Nanoscale 1-bit Full Adder at Wide Operating Temperatures. *NanoWorld J* 9(S5): S137-S142.

Copyright: © 2023 Nikhitha et al. This is an Open Access article distributed under the terms of the Creative Commons Attribution 4.0 International License (CCBY) (http://creativecommons.org/licenses/by/4.0/) which permits commercial use, including reproduction, adaptation, and distribution of the article provided the original author and source are credited.

Published by United Scientific Group

Abstract

1-Bit Full Adders (1-BFA) are the basic building blocks of advanced VLSI systems such as, micro and digital and signal processors. Therefore, here we report the driving capability and thermal reliability of 1-BFA designed using 16 nm CMOS process with a V_{DD} ranges from 0.7 V to 1.2 V. This 1-BFA is highly promising for the development of multi-stage structures because of their outstanding driving capability. The 16 nm CMOS process based 1-BFA exhibited a power and delay of 1.903 µW and 33.18 pS with a V_{DD} of 0.7 V @ 27 °C, whereas, it showcased a power and delay of 1.204 µW and 42.57 pS with a same V_{DD} @ 107 °C. When V_{DD} is escalated to 1.2 V, the 1-BFA showcased a power and delay of 46.53 µW and 3.193 pS @ 27 °C and 24.48 µW and 10.29 pS @ 107 °C, respectively.

Keywords

Carbon nanotube field effect transistor, Magnetic tunnel junction logic, Quantum dot cellular automata, Single electron transistor, Spin transfer torque logic

Introduction

A wide range of VLSI applications like microprocessors, video and image processing and digital signal processors broadly uses arithmetic operation such as multiplication, division, subtraction, addition and multiply and accumulate. 1-BFA is the basic building block of all these applications. Therefore, enhancing the performance of 1-BFA significantly improves the performance of VLSI systems [1-4]. With the tremendous growth in portable devices like laptops, cellular phones, tablets, note books, personal digital assist, personal communication systems and the evolution of the shrinking transistor technologies, the low power microelectronics research field has been boosted. Small area, low power, high throughput, high speed and energy efficiency are the key requirements in the development of VLSI systems [5, 6].

In recent years, MTJ, SET, CNTFET, and STT-based computing architectures have been reported [7-9]. In 2013, Breitkereutz et al. [10] reported a new technology called "perpendicular nanomagnetic logic" for the development of 1-BFAs. Transistor technologies and dimensions (W/L) significantly affects the performance of digital ICs and therefore, optimizing the W/L ratio of transistors is very important in achieving a low power delay product [11-13]. In 2022, Khan and Hasan [12] reported the development of a CMOS/MTJ- based hybrid approximate 1-BFA that offers excellent energy/are efficiency and high speed. In the same year, Ji et al. [13] reported the development of a CMOS full adder based ALU made using a-IGZO thin film transistor. Shukla et al. [14] also reported a

new CMOS/MTJ-based hybrid magnetic full adder in 2022, that showcased outstanding energy efficiency and reliability. In 2022, Rafiee et al. [15] demonstrated a high performance 1-BFA which is considered as a promising technology for the development of multistage VLSI structures due to its outstanding driving capability. In this work, we intensively investigated the thermal reliability and V_{DD} scaling effects on the performance of 1-BFA reported by Rafiee et al. [15].

Experimentation

Transmission gate based low power full adder

The TG (Transmission gate) based low power 1-BFA used in this study (Figure 1) is reported by Rafiee et al. [15] has a unique ability to generate full swing sum and output carry signals. This adder is suitable for developing multi-stage VLSI circuits such as multipliers, compressors and ripple carry adders (RCAs). The detailed operation of TG-based low power 1-BFA is reported in [15]. The 1-BFA is designed using 16 nm (PTM (predictive technology model)) CMOS process. The PMOS and NMOS devices had a width of 128 nm and 43 nm, respectively. The SPICE simulations were done at wide temperatures (From 27 ˚C to 107 ˚C) to study the thermal reliability of TG-based low power 1-BFA. This low power TG-based 1-BFA circuit is simulated with a V_{DD} ranging from 0.7 V to 1.2 V.

I-V Characteristics of 16 nm (PTM) CMOS process

Before implementing the low power TG-based 1-BFA, We studied the performance of PTM 16 nm NMOS and PMOS transistors. The gate widths of the PTM 16 nm NMOS/PMOS devices are fixed to 160 nm to study the performance. The devices showcased a threshold voltage of ±0.4 V. The PTM 16 nm NMOS showcased a drain current of around 75 µA and 300 µA at a drain bias of 0.1 V and 0.4 V, respectively. The gate voltage is swept from 0 to 1.2 V (Figure 2). The output curves (Figure 3) of PTM 16 nm NMOS indicates that the device maintain excellent pinch off behavior upto a drain bias of 1.2 V. The PTM 16 nm NMOS offered a drain current of 600 µA at a gate and drain bias of 1.2 V.

The PTM 16 nm PMOS showcased a drain current of around 50 µA and 180 µA at a drain bias of -0.1 V and -0.4 V, respectively. The gate voltage is swept from 0 to -1.2 V (Figure 4). The output curves of PTM 16 nm PMOS indicates that the device maintain excellent pinch off behavior upto a drain bias of -1.2 V (Figure 5). The PTM 16 nm PMOS offered a drain current of 430 µA at a gate and drain bias of -1.2 V.

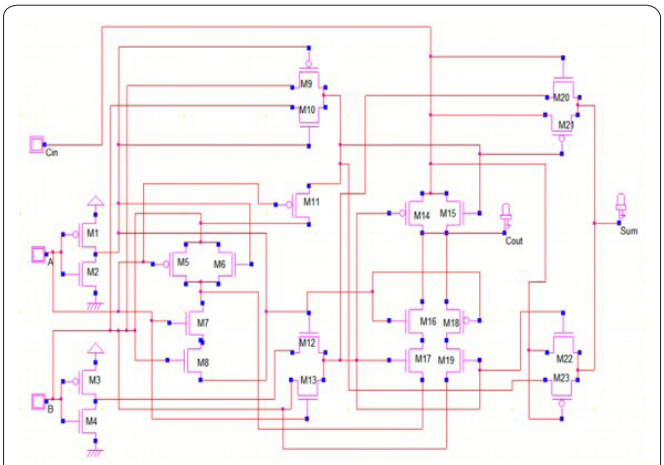

Figure 1: Transistor level diagram of TG-based low power 1-BFA [27].

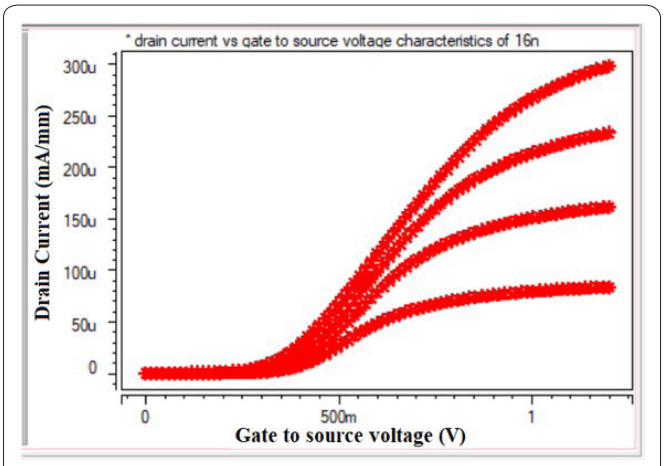

Figure 2: Transfer curves of PTM 16 nm NMOS with width = 160 nm.

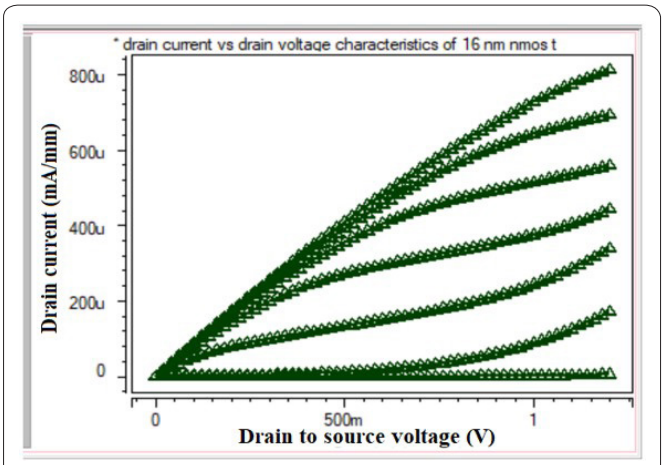

Figure 3: Output curves of PTM 16 nm NMOS with width = 160 nm.

Results and Discussion

1-BFA performance analysis

A combination of one multiplexer, one carry generator, one XOR gate, one XNOR gate, one AND gate and an inverter is used to construct the low power TG-based 1-BFA that offers full swing outputs. The output of the XOR and XNOR gates are the inputs to the multiplexer that generates sum output based on the input carry (select signal). A unique 6 transistor circuit is used by Rafiee et al. [15] to generate full swing carry output. If the width of PMOS (M18) is three times the width of NMOS (M19), the carry generator produces full swing output. But, in our work, we kept the width of all NMOS transistors the same. Therefore, full swing outputs weren't received with our simulations (Figure 6 and figure 7). The 1-BFA with a V_{DD} of 0.7 V offered a power and delay of 1.903 µW and 33.18 pS @ 27 ˚C and 1.204 µW and 42.57 pS @ 107 ˚C, respectively. That is when temperature is escalated from 27 ˚C to 107 ˚C, the power of 1-BFA is decreased by 36.73% and delay is increased by 22.06%. The short circuit power (P_{SC}) of TG-based low power 1-BFA designed with a V_{DD} of 0.7 V is 1.5 - 5.5 µW (27 ˚C - 107 ˚C) (Figure 8).

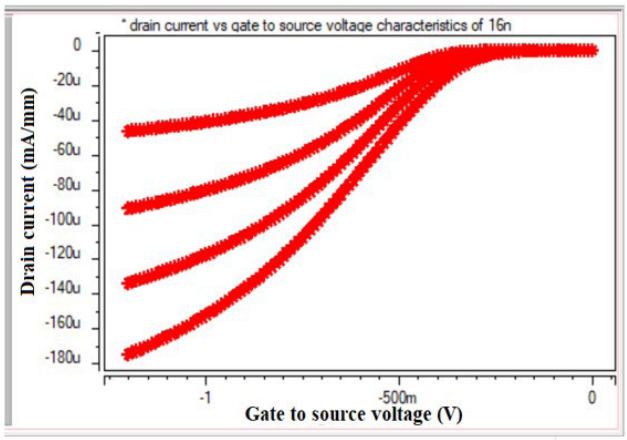

Figure 4: Transfer curves of PTM 16 nm PMOS with width = 160 nm.

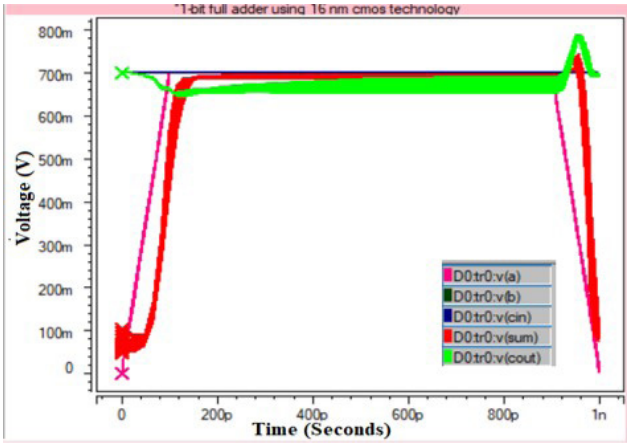

Figure 7: Transient waveforms of 1-BFA with V_{DD} = 0.7 V.

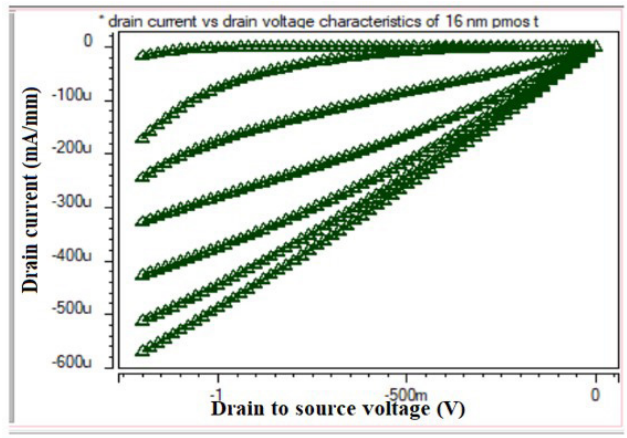

Figure 5: Output curves of PTM 16 nm PMOS with width = 160 nm.

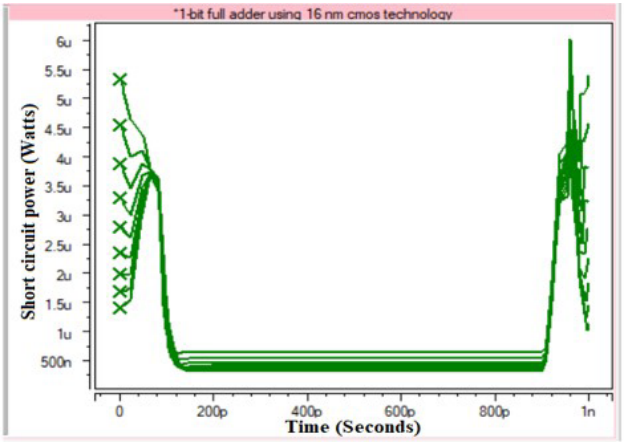

Figure 8: P_{SC} of 1-BFA with V_{DD} = 0.7 V.

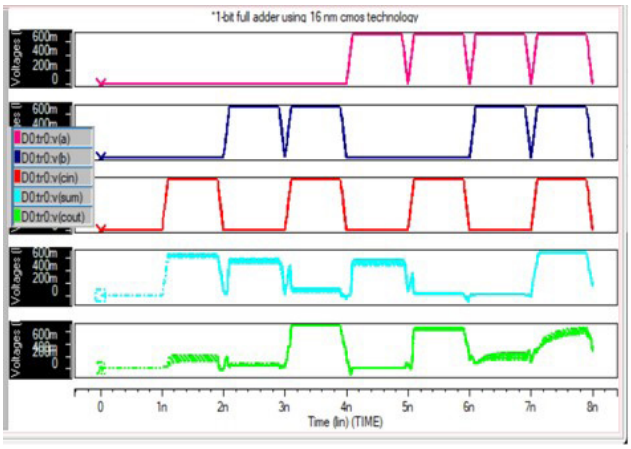

Figure 6: Transient response of TG-based low power 1-BFA.

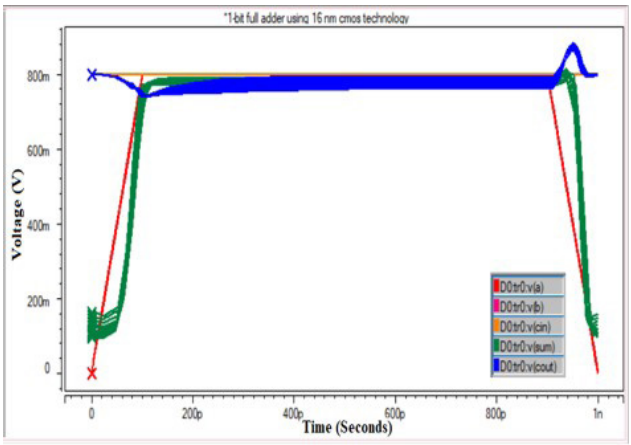

Figure 9: Transient waveforms of 1-BFA with V_{DD} = 0.8 V.

The 1-BFA with a V_{DD} of 0.8 V offered a power and delay of 4.420 µW and 22.83 pS @ 27 °C and 2.309 µW and 29.84 pS @ 107 °C, respectively (Figure 9). That is when temperature is escalated from 27 °C to 107 °C, the power of 1-BFA is decreased by 47.76 % and delay is increased by 23.49%. The P_{SC} of TG-based low power 1-BFA designed with a V_{DD} of 0.8 V is 3.6 - 10.4 µW (27 °C - 107 °C) (Figure 10). The 1-BFA with a V_{DD} of 0.9 V offered a power and delay of 9.789 µW and 16.62 pS @ 27 °C and 4.558 µW and 22.12 pS @ 107 °C, respectively (Figure 11). That is when temperature is escalated from 27 °C to 107 °C, the power of 1-BFA is decreased by 53.44% and delay is increased by 24.49%. The P_{SC} of TG-based low power 1-BFA designed with a V_{DD} of 0.9 V is 6.8 - 20 µW (27 °C - 107 °C) (Figure 12).

The 1-BFA with a V_{DD} of 1.0 V offered a power and delay of 18.58 µW and 10.63 pS @ 27 °C and 8.664 µW and 17.31 pS @ 107 °C, respectively (Figure 13). That is when temperature is escalated from 27 °C to 107 °C, the power of 1-BFA is decreased by 53.37% and delay is increased by 38.59%. The P_{SC} of TG-based low power 1-BFA designed with a V_{DD} of

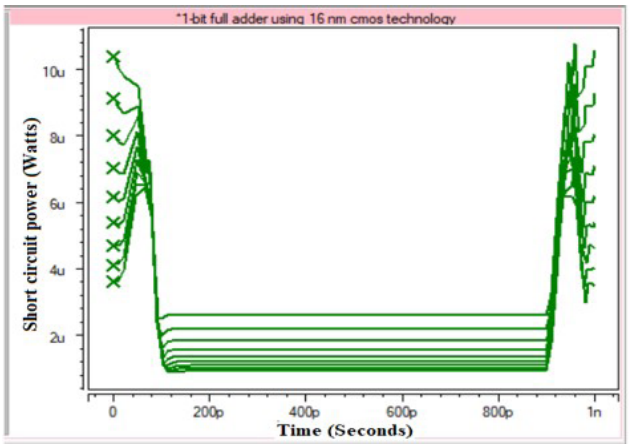

Figure 10: P_{SC} of 1-BFA with V_{DD} = 0.8 V.

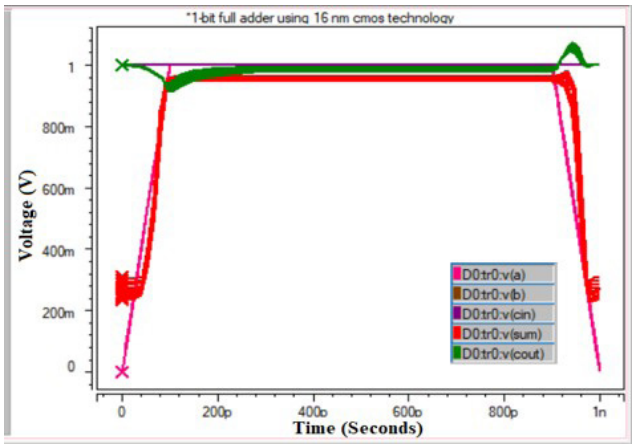

Figure 13: Transient waveforms of 1-BFA with V_{DD} = 1.0 V.

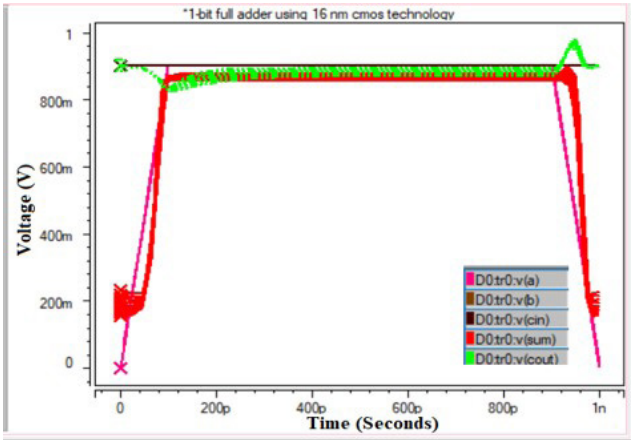

Figure 11: Transient waveforms of 1-BFA with V_{DD} = 0.9 V.

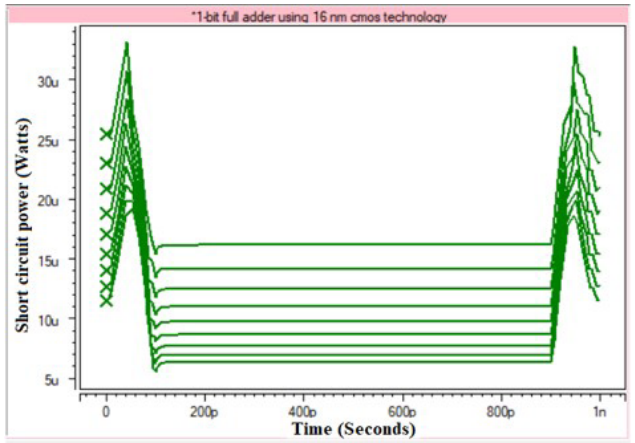

Figure 14: P_{SC} of 1-BFA with V_{DD} = 1.0 V.

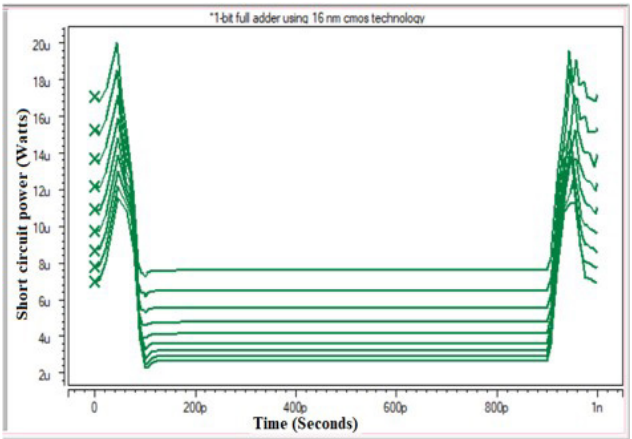

Figure 12: P_{SC} of 1-BFA with V_{DD} = 0.9 V.

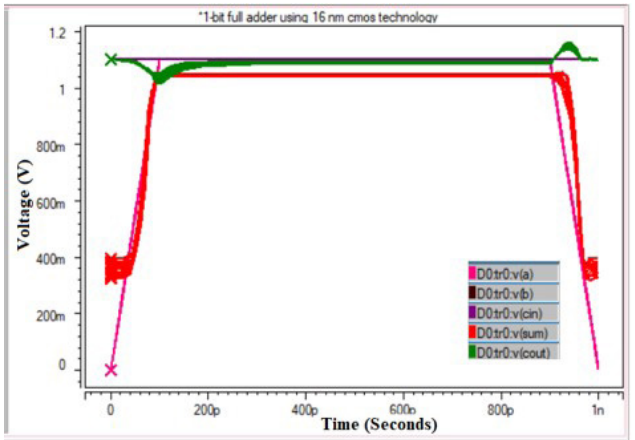

Figure 15: Transient waveforms of 1-BFA with V_{DD} = 1.1 V.

1.0 V is 11 - 33 µW (27 °C - 107 °C) (Figure 14). The 1-BFA with a V_{DD} of 1.1 V offered a power and delay of 30.91 µW and 8.047 pS @ 27 °C and 15.24 µW and 13.72 pS @ 107 °C, respectively (Figure 15). That is when temperature is escalated from 27 °C to 107 °C, the power of 1-BFA is decreased by 50.70% and delay is increased by 41.35%. The P_{SC} of TG-based low power 1-BFA designed with a V_{DD} of 1.0 V is 17 - 49 µW (27 °C - 107 °C) (Figure 16). Finally, the 1-BFA with a V_{DD} of 1.2 V offered a power and delay of 46.53 µW and 3.193 pS @ 27 °C and 24.48 µW and 10.29 pS @ 107 °C, respectively (Figure 17). That is when temperature is escalated from 27 °C to 107 °C, the power of 1-BFA is decreased by 47.39% and delay is increased by 68.97%. The P_{SC} of TG-based low power 1-BFA designed with a V_{DD} of 1.2 V is 24 - 67 µW (27 °C - 107 °C) (Figure 18). TG-based low power 1-BFA made with 16 nm technology and a V_{DD} of 0.7 V is thermally stable. At large V_{DD}, the deviation in delay and power with temperature is more (Figure 19).

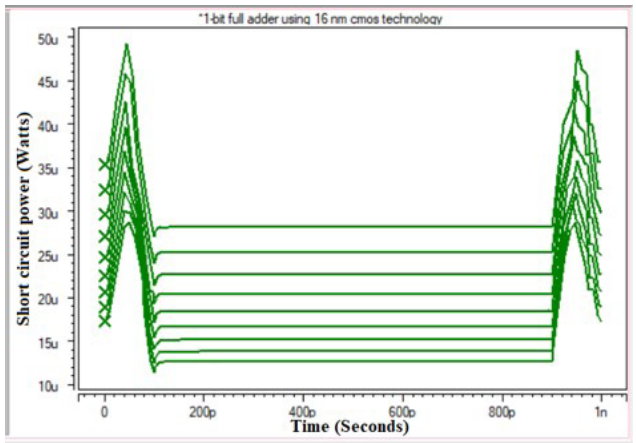

Figure 16: P_{SC} of 1-BFA with V_{DD} = 1.1 V.

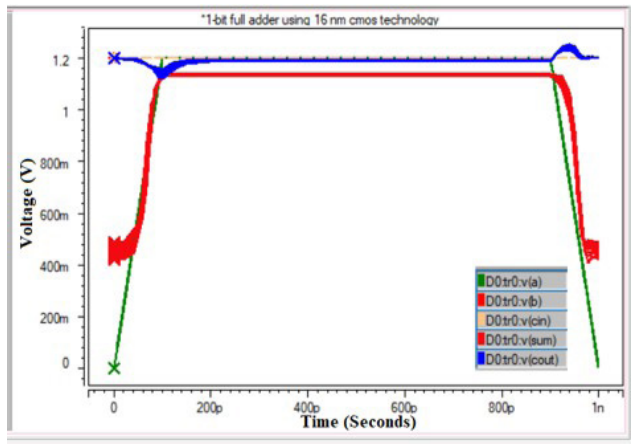

Figure 17: Transient waveforms of 1-BFA with V_{DD} = 1.2 V.

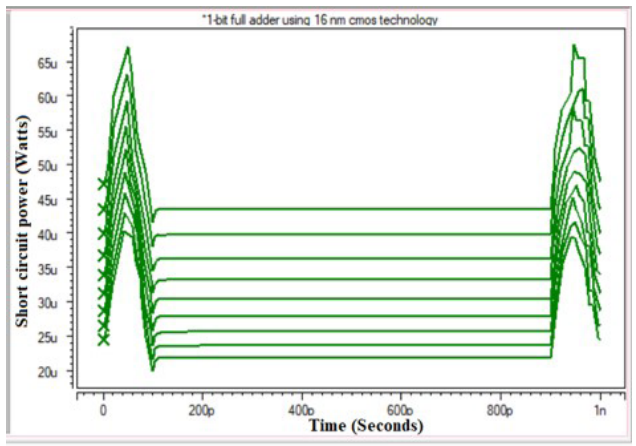

Figure 18: P_{SC} of 1-BFA with V_{DD} = 1.2 V.

In order to analyze the driving capability of TG-based low power 1-BFA, we developed a 4-bit RCA (Figure 20) with 16 nm CMOS process and a V_{DD} of 0.7 V. The 4-bit RCA exhibited full swing outputs and at 27 °C, the 4-bit RCA offered a power and delay of 3.099 µW and 132.72 pS, respectively. Table 1 provides the thermal effects on the delay and power of 4-bit RCA designed using TG-based low power 1-BFA.

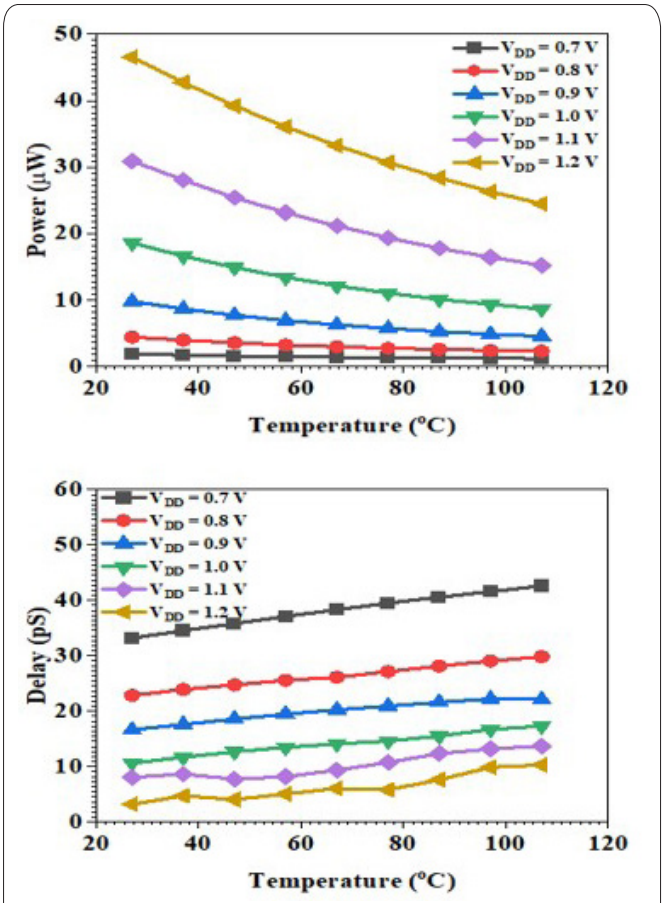

Figure 19: Thermal/V_{DD} scaling effects on delay and power of 1-BFA.

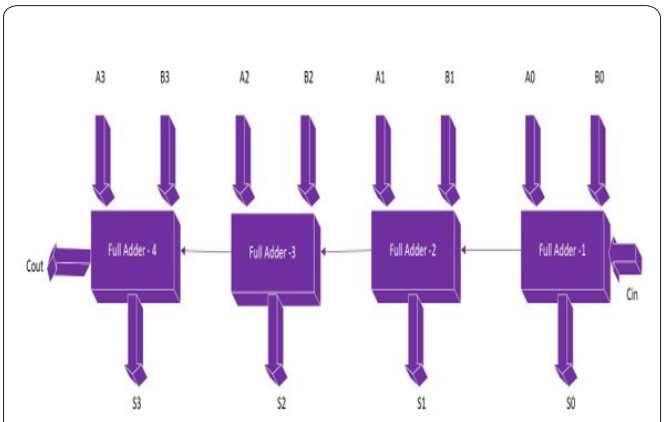

Figure 20: 4-bit RCA schematic.

Conclusion

In this work, we studied the driving capability and thermal reliability of low power TG-based 1-BFA designed using PTM 16 nm CMOS Process with a V_{DD} ranging from 0.7 V to 1.2 V. The low power TG-based 1-BFA with 0.7 V supply, offered a power and delay of 1.903 µW and 33.18 pS and 1.204 µW and 42.57 pS, respectively @ 27 °C and 107 °C. When supply voltage is escalated to 1.2 V, the low power TG-based 1-BFA offered a power and delay of 46.53 µW and 3.193 pS and 24.48 µW and 10.29 pS, respectively @ 27 °C and 107 °C. The 4-bit RCA designed using low power TG-based

Table 1: Performance of TG-1-BFA-based 4-bit RCA.

Temperature (°C)	Parameters	
	Power (μW)	Delay (pS)
27	3.099	132.72
37	2.714	138.08
47	2.415	143.28
57	2.209	148.36
67	2.071	153.24
77	1.959	158
87	1.888	162.4
97	1.845	166.52
107	1.821	170.48

1-BFA exhibited full swing outputs and at 27 °C/107 °C, the 4-bit RCA offered a power and delay of 3.099 μW/1.821 μW and 132.72 pS/170.48 pS, respectively.

Acknowledgements

None.

Conflict of Interest

None.

References

1. Bhattacharyya P, Kundu B, Ghosh S, Kumar V, Dandapat A. 2014. Performance analysis of a low-power high-speed hybrid 1-bit full adder circuit. *IEEE Trans Very Large Scale Integr VLSI Syst* 23(10): 2001-2008. https://doi.org/10.1109/TVLSI.2014.2357057
2. Mehrabani YS, Eshghi M. 2016. Noise and process variation tolerant, low-power, high-speed, and low-energy full adders in CNFET technology. *IEEE Trans Very Large Scale Integr VLSI Syst* 24(11): 3268-3281. https://doi.org/10.1109/TVLSI.2016.2540071
3. Waris H, Wang C, Liu W, Han J, Lombardi F. 2020. Hybrid partial product-based high-performance approximate recursive multipliers. *IEEE Trans Emerg Top* 10(1): 507-513. https://doi.org/10.1109/TETC.2020.3013977
4. Ansari MS, Cockburn BF, Han J. 2020. Low-power approximate logarithmic squaring circuit design for DSP applications. *IEEE Trans Emerg Top* 10(1): 500-506. https://doi.org/10.1109/TETC.2020.2989699
5. Jiang Y, Al-Sheraidah A, Wang Y, Sha E, Chung JG. 2004. A novel multiplexer-based low-power full adder. *IEEE Trans Circuits Syst II Express Briefs* 51(7): 345-348. https://doi.org/10.1109/TCSII.2004.831429
6. Hasan M, Hossein MJ, Hossain M, Zaman HU, Islam S. 2019. Design of a scalable low-power 1-bit hybrid full adder for fast computation. *IEEE Trans Circuits Syst II Express Briefs* 67(8): 1464-1468. https://doi.org/10.1109/TCSII.2019.2940558
7. Jin X, Chen W, Li X, Yin N, Wan C, et al. 2022. High-reliability, reconfigurable, and fully non-volatile full-adder based on SOT-MTJ for image processing applications. *IEEE Trans Circuits Syst II Express Briefs* 70(2): 781-785. https://doi.org/10.1109/TCSII.2022.3213747
8. Li X, Jin X, Chen W, Yin N, Yu Z. 2022. Parallel-prefix adder in spin-orbit torque magnetic RAM for high bit-width non-volatile computation. *IEEE Trans Circuits Syst II Express Briefs* 70(2): 761-765. https://doi.org/10.1109/TCSII.2022.3214504
9. Raouf M, Timarchi S. 2023. Non-volatile and high-performance cascadable spintronic full-adder with no sensitivity to input scheduling. *IEEE Trans Circuits Syst II Express Briefs* 70(6): 2236-2240. https://doi.org/10.1109/TCSII.2023.3237855
10. Breitkreutz S, Kiermaier J, Eichwald I, Hildbrand C, Csaba G, et al. 2013. Experimental demonstration of a 1-bit full adder in perpendicular nanomagnetic logic. *IEEE Trans Magn* 49(7): 4464-4467. https://doi.org/10.1109/TMAG.2013.2243704
11. Naseri H, Timarchi S. 2018. Low-power and fast full adder by exploring new XOR and XNOR gates. *IEEE Trans Very Large Scale Integr VLSI Syst* 26(8): 1481-1493. https://doi.org/10.1109/TVLSI.2018.2820999
12. Khan MA, Hasan M. 2022. Design of high speed, energy, and area efficient spin-based hybrid MTJ/CMOS and CMOS only approximate adders. *IEEE Trans Magn* 58(5): 1-8. https://doi.org/10.1109/TMAG.2022.3155968
13. Ji H, Geng D, Chuai X, Duan X, Chen Q, et al. 2022. An advanced full adder based arithmetic logic unit (ALU) using low-temperature poly-si oxide TFTs. *IEEE Trans Electron Dev* 69(11): 6160-6165. https://doi.org/10.1109/TED.2022.3208074
14. Shukla P, Kumar P, Misra PK. 2022. An energy efficient, mismatch tolerant offset compensating hybrid MTJ/CMOS magnetic full adder. *IEEE Trans. Circuits Syst II Express Briefs* 69(11): 4548-4552. https://doi.org/10.1109/TCSII.2022.3190455
15. Rafiee M, Shiri N, Sadeghi A. 2021. High-performance 1-bit full adder with excellent driving capability for multistage structures. *IEEE Embed Syst Lett* 14(1): 47-50. https://doi.org/10.1109/LES.2021.3108474